Relativistic light shifts in hydrogenlike ions

Octavian Postavaru
Center for Research and Training in Innovative Techniques of Applied Mathematics in Engineering, University Politehnica of Bucharest, Splaiul Independentei 313, Bucharest 060042, Romania

(Received 27 July 2022; accepted 4 January 2023; published 13 January 2023)

We investigate the level structure of heavy hydrogenlike ions in laser beams. In heavy ions, the electrons are tightly bound by the Coulomb potential of the nucleus, which prohibits ionization even by strong lasers. However, interaction with the light field leads to dynamic shifts of the electronic energy levels. We apply a fully relativistic description of the electronic states by means of the Dirac equation. Interaction with the monofrequent laser field is treated by second-order time-dependent perturbation theory. Our formalism goes beyond the Stark long-wavelength dipole approximation and takes into account nondipole effects of retardation and interaction with the magnetic-field components of the laser beam. The resulting level shifts are relevant for experiments at present and near-future laser facilities.

DOI: 10.1103/PhysRevA.107.013105

I. INTRODUCTION

Laser spectroscopy of atomic systems has been greatly contributing to our understanding of nature [1]. The investigation of transition energies in hydrogen yielded the most accurate value for a physical quantity ever measured. Frequency comb techniques have led to the construction of all-optical atomic clocks of unprecedented accuracy [2] and enable the observation of the expansion of the universe in real time by measuring the cosmological redshift of distant astronomical objects [3].

Two-photon absorption (TPA) is of fundamental importance in super-resolution imaging and spectroscopy. Isotope shifts were determined by two-photon Doppler-free spectroscopy and by collinear laser spectroscopy [4,5], providing valuable insight into the collective structure of nuclei. Recently, the paper [6] reports an absolute frequency measurement of the $2s3d\ ^1D_2$ state in neutral ^{9}Be. In the paper [7], the authors consider nonresonant corrections to $2s - ns/nd$ transition frequencies in hydrogen for the experiments based on two-photon spectroscopy, concluding that the corrections could be significant for the determination of Rydberg constant and proton charge radius. In the paper [8], the authors develop a theoretical framework for spin selection in single-frequency two-photon excitation of alkali-metal atoms as a function of polarization of the excitation light, and verify the theory by experimentally probing the $3S_{1/2} \rightarrow 6S_{1/2}$ transition rate in ^{87}Rb.

TPA has potential applications in quantum information processing. The paper [9] studies multiphoton blockade and photon-induced tunneling effects in the two-photon Jaynes-Cummings model, concluding that quantum interference can enhance the photon blockade effect. The work [6] demonstrates a simple method to generate a broader and flatter orbital angular momentum spectrum of entangled photon pairs by modifying the pump beam profile.

Energy shifts of atomic levels due to laser fields play an important role in high-precision laser spectroscopy. The dynamic Stark shift is one of the inherent systematic effects that shifts atomic energy levels in a laser spectroscopic experiment. In contrast to other shifting effects which may in principle be experimentally controllable, the dynamic Stark shift is due to the probing laser field itself and as such it cannot be eliminated. The dynamic (ac) Stark shift is also present in laser-induced processes like ionization [10–12]. Theoretical investigations so far apply nonrelativistic approaches and are restricted to electric dipole interactions.

In this paper we calculate light field shifts in single-electron ions in a fully relativistic manner. Compared to the works [13,14], the bare atomic states are solutions of the Dirac equation rather than Schrödinger's equation. The interaction with the monofrequent laser field is treated by perturbation theory in the second order. Relativistic calculations of the dynamic dipole polarizability for the ground state of hydrogenic ions have been undertaken before [15]. In this paper, beyond dipole effects, the relativistic effects of retardation and level shifts due to interaction of the magnetic component of the laser—ac Zeeman shifts—are accounted for. Furthermore, we generalize previous investigations to the case of excited states with substantially larger level shifts. With our approach, not only does the accuracy of calculated level shifts increase, but, it also allows one to extend the field of investigations to stronger laser fields and higher frequencies, e.g., x-ray lasers [16]. As relativistic effects scale with high powers of the charge number Z, the theoretical description of atomic systems of the highest nuclear charges is accessible this way.

This paper is structured as follows. In Sec. II, we briefly summarize the derivation of the energy shift expression from perturbation theory and extend the standard method to the relativistic case. In Sec. III, the decomposition of the matrix elements into angular and radial integrals is presented. The resulting expressions are evaluated by algebraic and analytical

means. In Sec. IV, we discuss numerical results for some selected systems of interest. Finally, we conclude the paper with a summary. Some auxiliary calculations are given in the Appendix.

II. DYNAMIC SHIFT BY MEANS OF PERTURBATION THEORY

Let us consider the effect of adding the interaction Hamiltonian $V(\epsilon,t)$ to the sum of relativistic hydrogenlike ion H_0:

$$\begin{aligned} H &= H_0 + V(\epsilon,t), \\ H_0 &= c\boldsymbol{\alpha}\boldsymbol{p} + \boldsymbol{\beta}m_0c^2 - \frac{Ze^2}{4\pi\epsilon_0 r}, \\ V(\epsilon,t) &= -(A_0\boldsymbol{\alpha}\hat{\epsilon}_\nu e^{i\boldsymbol{k}\boldsymbol{r}-i\omega t} + \text{c.c.})e^{\epsilon t}. \end{aligned} \tag{1}$$

Here, ϵ is an infinitesimal damping parameter [17]. The introduction of an adiabatic damping parameter is a key element of time-dependent perturbation theory. In the interaction picture (denoted by the subscript I), the interaction V is represented by [18]

$$V_I(\epsilon,t) = e^{\frac{i}{\hbar}H_0 t}V(\epsilon,t)e^{-\frac{i}{\hbar}H_0 t}. \tag{2}$$

We calculate the time evolution operator U_I up to second order in V_I from the Dyson series:

$$\begin{aligned} U_I &= \lim_{t\to\infty} U_I(\epsilon,t), \\ U_I(\epsilon,t) &= 1 - \frac{i}{\hbar}\int_{-\infty}^{t} dt' V_I(\epsilon,t) + \left(-\frac{i}{\hbar}\right)^2 \\ &\quad\times \int_{-\infty}^{t} dt' \int_{-\infty}^{t} dt'' V_I(\epsilon,t')V_I(\epsilon,t''). \end{aligned} \tag{3}$$

Let Φ_n represent an eigenfunction of the unperturbed Hamiltonian H_0 with an eigenvalue E_n. We denote the complete set of eigenstates of H_0 by $\{|\Phi_n\rangle\}$. $|\Phi_I(t)\rangle$ is a time-dependent atomic state in the interaction picture. The state function before interaction is an eigenstate of H_0: $|\Phi_I(t=-\infty)\rangle = |\Phi_a\rangle$, where Φ_a is an eigenstate of the unperturbed Hamiltonian H_0. Thus the state function at any time can be constructed by applying the evolution operator as

$$|\Phi_I(t)\rangle = U_I(\epsilon,t)|\Phi_I(t=-\infty)\rangle = \sum_n c_n(t)|\Phi_n\rangle. \tag{4}$$

This condition is also true for the degenerate case [18] without loss of generality. The time-dependent expansion coefficients $c_n(t)$ are given as the projections

$$c_n(t) = \langle\Phi_n|\Phi_I(t)\rangle. \tag{5}$$

For calculating the light shift of a given atomic state a, we are interested in the projection [17]

$$c_a(t) = \langle\Phi_a|\Phi_I(t)\rangle = \langle\Phi_a|U_I(\epsilon,t)|\Phi_a\rangle. \tag{6}$$

The first-order perturbation $\langle\Phi_a|V|\Phi_a\rangle$ vanishes. Substituting $U_I(\epsilon,t)$ from Eq. (3), the leading order of the perturbation expansion is V^2 and the problem reduces to calculating the matrix element

$$\begin{aligned} M &= \int_{-\infty}^{t} dt' \int_{-\infty}^{t'} dt'' \langle\Phi_a|V_I(\epsilon,t')V_I(\epsilon,t'')|\Phi_a\rangle \\ &= \sum_n \int_{-\infty}^{t} dt' \int_{-\infty}^{t'} dt'' \langle\Phi_a|V_I(\epsilon,t')|\Phi_n\rangle \\ &\quad\times \langle\Phi_n|V_I(\epsilon,t'')|\Phi_a\rangle. \end{aligned} \tag{7}$$

The index n counts all bound and continuum states of the unperturbed hydrogenlike ion. After carrying out the time integration, the matrix element is given as

$$\begin{aligned} M = -\frac{\hbar}{i}\sum_n \Bigg(& A_0^2 \frac{\langle\Phi_a|V_1|\Phi_n\rangle\langle\Phi_n|V_1|\Phi_a\rangle e^{2t(\epsilon-i\omega)}}{2(\epsilon-i\omega)(E_a-E_n+\hbar\omega-i\hbar\epsilon)} \\ & + |A_0|^2 \frac{\langle\Phi_a|V_2|\Phi_n\rangle\langle\Phi_n|V_1|\Phi_a\rangle}{2\epsilon(E_a-E_n-\hbar\omega-i\hbar\epsilon)} e^{2\epsilon t} \\ & + |A_0|^2 \frac{\langle\Phi_a|V_1|\Phi_n\rangle\langle\Phi_n|V_2|\Phi_a\rangle}{2\epsilon(E_a-E_n+\hbar\omega-i\hbar\epsilon)} e^{2\epsilon t} \\ & + (A_0^*)^2 \frac{\langle\Phi_a|V_2|\Phi_n\rangle\langle\Phi_n|V_2|\Phi_a\rangle e^{2t(\epsilon+i\omega)}}{2(\epsilon+i\omega)(E_a-E_n-\hbar\omega-i\hbar\epsilon)} \Bigg). \end{aligned} \tag{8}$$

For simplicity the notation $V_1 = -\boldsymbol{\alpha}\hat{\epsilon}_\nu e^{i\boldsymbol{k}\boldsymbol{r}}$ and $V_2 = -\boldsymbol{\alpha}^*\hat{\epsilon}_\nu^* e^{-i\boldsymbol{k}\boldsymbol{r}}$ is introduced above. In the second order of perturbation theory one can write

$$c_a(t) = -\frac{i}{\hbar}M'(t), \tag{9}$$

with $M' = -\frac{i}{\hbar}M$. Neglecting higher-order terms, the logarithmic derivative of the expansion coefficient is

$$\frac{d}{dt}\ln[c_a(t)] = -\frac{i}{\hbar}\frac{dM'}{dt}. \tag{10}$$

In the limit $\epsilon\to 0$, the time derivative of the matrix element is

$$\begin{aligned} \frac{dM'}{dt} = \sum_n \Bigg(& A_0^2 \frac{\langle\Phi_a|V_1|\Phi_n\rangle\langle\Phi_n|V_1|\Phi_a\rangle}{E_a-E_n+\hbar\omega} e^{-2i\omega t} \\ & + |A_0|^2 \frac{\langle\Phi_a|V_2|\Phi_n\rangle\langle\Phi_n|V_1|\Phi_a\rangle}{E_a-E_n-\hbar\omega} \\ & + |A_0|^2 \frac{\langle\Phi_a|V_1|\Phi_n\rangle\langle\Phi_n|V_2|\Phi_a\rangle}{E_a-E_n+\hbar\omega} \\ & + (A_0^*)^2 \frac{\langle\Phi_a|V_2|\Phi_n\rangle\langle\Phi_n|V_2|\Phi_a\rangle}{E_a-E_n-\hbar\omega} e^{2i\omega t} \Bigg). \end{aligned} \tag{11}$$

For $\omega\neq 0$ we use the property $e^{2i\omega t} = \frac{1}{2i\omega}\int_0^t dt' e^{2i\omega t'}$. Using relation (3) (see [19]) to form the Dyson series, we get

$$\begin{aligned} \frac{dM'}{dt} = \sum_n \Bigg(& |A_0|^2 \frac{\langle\Phi_a|V_2|\Phi_n\rangle\langle\Phi_n|V_1|\Phi_a\rangle}{E_a-E_n-\hbar\omega} \\ & + |A_0|^2 \frac{\langle\Phi_a|V_1|\Phi_n\rangle\langle\Phi_n|V_2|\Phi_a\rangle}{E_a-E_n+\hbar\omega} \Bigg). \end{aligned} \tag{12}$$

Because $\frac{dM'}{dt}$ is time independent, one can make the ansatz [17]

$$\frac{\dot{c}_a}{c_a} = -\frac{i}{\hbar}\Delta E, \tag{13}$$

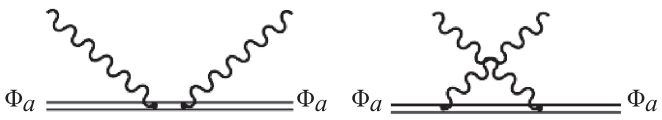

FIG. 1. Diagrams representing the lowest-order perturbative light shift corrections. The Coulomb-dressed electron is depicted by a double line and the wavy lines represent photons.

and define the energy shift of the state a due to interaction with the light field as

$$\Delta E = |A_0|^2 \sum_n \left(\frac{\langle \Phi_a|V_2|\Phi_n\rangle\langle\Phi_n|V_1|\Phi_a\rangle}{E_a - E_n - \hbar\omega} + \frac{\langle \Phi_a|V_1|\Phi_n\rangle\langle\Phi_n|V_2|\Phi_a\rangle}{E_a - E_n + \hbar\omega} \right). \tag{14}$$

A_0 is given as $|A_0|^2 = \frac{|\boldsymbol{E}|^2 c^2}{\omega^2}$, with $\boldsymbol{E}$ being the electric-field strength. In Fig. 1, the diagrams representing the two terms in the above equations are shown.

III. EVALUATION OF MATRIX ELEMENTS

In this section we describe how the relativistic wave functions, the vector potential of the electromagnetic field, and the interaction matrix elements in Eq. (14) are treated. Our description is fully relativistic and accounts for spin and magnetic-field effects. A similar description is used for the relativistic theoretical study of the spontaneous emission in [19–22].

The principal task in calculating the light shift is the evaluation of the matrix element:

$$M = \sum_n \frac{\langle \Phi_a|\hat{\alpha}\hat{\epsilon}_\nu^* e^{-i\boldsymbol{kr}}|\Phi_n\rangle\langle\Phi_n|\hat{\alpha}\hat{\epsilon}_\nu e^{i\boldsymbol{kr}}|\Phi_a\rangle}{E_a - E_n - \hbar\omega}. \tag{15}$$

We apply the multipole decomposition of the transverse electromagnetic plane wave as

$$\hat{\alpha}\hat{\epsilon}_\nu e^{i\boldsymbol{kr}} = 4\pi\hat{\alpha}\sum_{lm}\sum_{\lambda=0}^{1} i^{l-\lambda}[\boldsymbol{Y}_{lm}^{(\lambda)}(\hat{k})\cdot\hat{\epsilon}_\nu]^\dagger \boldsymbol{a}_{lm}^{(\lambda)}(\boldsymbol{r}), \tag{16}$$

thus M becomes

$$M = 16\pi^2 \sum_{nlm\lambda l'm'\lambda'} \langle\Phi_a|\hat{\alpha}^* i^{\lambda-l}[\hat{\epsilon_\nu}\boldsymbol{Y}_{lm}^{(\lambda)}(\hat{k})]\boldsymbol{a}_{lm}^{(\lambda)\dagger}(\boldsymbol{r})|\Phi_n\rangle \times \frac{\langle\Phi_n|\hat{\alpha}(i^*)^{l'-\lambda'}(\boldsymbol{Y}_{l'm'}^{(\lambda')}(\hat{k})\hat{\epsilon_\nu})^\dagger \boldsymbol{a}_{l'm'}^{(\lambda')}(\boldsymbol{r})|\Phi_a\rangle}{E_a - E_n - \hbar\omega}. \tag{17}$$

To obtain the level shift, a summation over polarization states and integration over photon directions have to be performed:

$$\bar{M} = \frac{1}{2}\sum_\nu \frac{1}{4\pi}\int d\Omega_k M. \tag{18}$$

However, for simplicity we drop the overbar of M from here on. Using the orthogonality property

$$\sum_\nu \int d\Omega_k [\boldsymbol{Y}_{l'm'}^{(\lambda')}(\hat{k})\hat{\epsilon}_\nu]^\dagger[\hat{\epsilon_\nu}\boldsymbol{Y}_{lm}^{(\lambda)}(\hat{k})] = \delta_{ll'}\delta_{mm'}\delta_{\lambda\lambda'}, \tag{19}$$

the expression above simplifies to

$$M = 2\pi\sum_{nlm\lambda}\frac{\langle\Phi_a|\hat{\alpha}^*\boldsymbol{a}_{lm}^{(\lambda)\dagger}(\boldsymbol{r})|\Phi_n\rangle\langle\Phi_n|\hat{\alpha}\boldsymbol{a}_{lm}^{(\lambda)}(\boldsymbol{r})|\Phi_a\rangle}{E_a - E_n - \hbar\omega}. \tag{20}$$

Using the spectral representation of Green's function

$$G(\boldsymbol{r},\boldsymbol{r}';z) = \sum_n \frac{\Phi_n(\boldsymbol{r})\Phi_n(\boldsymbol{r})^\dagger}{E_n - z}, \tag{21}$$

and splitting Eq. (20) into an electric ($\lambda = 1$) and a magnetic ($\lambda = 0$) part we get

$$M = -2\pi\sum_{lm}\int d\boldsymbol{r}d\boldsymbol{r}'\Phi_a^\dagger(\boldsymbol{r})\hat{\alpha}^*\boldsymbol{a}_{lm}^{(0)\dagger}(\boldsymbol{r})G(\boldsymbol{r},\boldsymbol{r}';z) \times\hat{\alpha}\boldsymbol{a}_{lm}^{(0)}(\boldsymbol{r})\Phi_a(\boldsymbol{r}') - 2\pi\sum_{lm}\int d\boldsymbol{r}d\boldsymbol{r}'\Phi_a^\dagger(\boldsymbol{r})\hat{\alpha}^* \times\boldsymbol{a}_{lm}^{(1)\dagger}(\boldsymbol{r})G(\boldsymbol{r},\boldsymbol{r}';z)\hat{\alpha}\boldsymbol{a}_{lm}^{(1)}(\boldsymbol{r})\Phi_a(\boldsymbol{r}'), \tag{22}$$

where the energy variable is $z = E_a - \hbar\omega$.

We perform a gauge transformation of the matrix elements. The transformed multipole potential can be written as

$$\boldsymbol{a}_{JM}^{\lambda}(\hat{r}) \longrightarrow \boldsymbol{a}_{JM}^{\lambda}(\hat{r}) + \nabla\chi_{JM}(\hat{r}), \quad \Phi_{JM}(\hat{r}) \longrightarrow i\omega\chi_{JM}(\hat{r}), \tag{23}$$

where the gauge function $\chi_{JM}(\hat{r})$ (and the multipole potential) is a solution to the Helmholtz equation. We choose the gauge function to be

$$\chi_{JM}(\hat{r}) = -\frac{1}{k}G_J j_J(kr)Y_{JM}(\hat{r}). \tag{24}$$

With the choice of $G_J = \sqrt{J+1/J}$, the so-called Babushkin gauge, i.e., a relativistic generalization of the length form interaction, is adopted [21–23]. This transformation has no effect on the magnetic multipole potentials, but transforms electric potentials to the form

$$\boldsymbol{a}_{JM}^{(1)}(\hat{r}) = -j_{J+1}(kr)\left(\boldsymbol{Y}_{JM}^{(1)}(\hat{r}) - \sqrt{\frac{J+1}{J}}\boldsymbol{Y}_{JM}^{(-1)}(\hat{r})\right), \quad \Phi_{JM}^{(1)}(\hat{r}) = -ic\sqrt{\frac{J+1}{J}}j_J(kr)Y_{JM}(\hat{r}). \tag{25}$$

The electric multipole potentials can be rewritten as

$$\boldsymbol{a}_{JM}^{(1)}(\hat{r}) = -\sqrt{\frac{2J+1}{J}}\boldsymbol{a}_{JJ+1M}(\hat{r}), \tag{26}$$

with $\boldsymbol{a}_{JJ+1M}(\hat{r})$ given by Eq. (B7) in the Appendix.

Denoting with M^m the magnetic part and with M^e the electric part, after some algebraic manipulations we obtain

$$M^m = \frac{4\pi}{\hbar c}\sum_{lm\kappa_n}\{(R_1^m + R_4^m)K_{JJM}^{\kappa_n-\kappa_a}K_{JJM}^{-\kappa_n\kappa_a} - R_2^m\left(K_{JJM}^{-\kappa_n\kappa_a}\right)^2 - R_3^m\left(K_{JJM}^{\kappa_n-\kappa_a}\right)^2\},$$

$$M^e = \frac{4\pi}{\hbar c}\sum_{lm\kappa_n}\left\{\frac{2J+1}{J}\left[(R_1^e + R_4^e)K_{JJ+1M}^{\kappa_n-\kappa_a}K_{JJ+1M}^{-\kappa_n\kappa_a} - R_2^e\left(K_{JJ+1M}^{-\kappa_n\kappa_a}\right)^2 - R_3^e\left(K_{JJ+1M}^{\kappa_n-\kappa_a}\right)^2\right] - \frac{J+1}{J}\left[R_{1'}^e\left(K_{JM}^{\kappa_n\kappa_a}\right)^2 + (R_{2'}^e + R_{3'}^e)K_{JM}^{\kappa_n\kappa_a}K_{JM}^{-\kappa_n-\kappa_a} + R_{4'}^e\left(K_{JM}^{-\kappa_n-\kappa_a}\right)^2\right]\right\}. \tag{27}$$

We shall refer to the K's as the angular matrix elements and to the R's as the radial matrix elements.

The matrix element

$$M' = \sum_n \frac{\langle\Phi_a|\hat{\alpha}\hat{\epsilon}_\nu e^{i\boldsymbol{kr}}|\Phi_n\rangle\langle\Phi_n|\hat{\alpha}^*\hat{\epsilon}^*_\nu e^{-i\boldsymbol{kr}}|\Phi_a\rangle}{E_a - E_n + \hbar\omega}, \tag{28}$$

can readily be found from Eq. (27) by the substitutions $K^{\kappa_n-\kappa_a} \to K^{-\kappa_a-\kappa_n}$, $K^{\kappa_n\kappa_a} \to K^{\kappa_a-\kappa_n}$, $K^{\kappa_n\kappa_a} \to K^{\kappa_a\kappa_n}$, and $K^{-\kappa_n-\kappa_a} \to K^{-\kappa_a-\kappa_n}$. In the radial part, the energy variable $z = E_a + \hbar\omega$ has to be substituted.

A. Radial matrix elements

The following notations are introduced for the two-dimensional radial integrals:

$$\begin{aligned}
R^m_1 &= \int drdr' r^2 r'^2 F_a(r) j_J(kr) g_{12}(r,r';E) j_J(kr') G_a(r'),\\
R^m_2 &= \int drdr' r^2 r'^2 G_a(r) j_J(kr) g_{22}(r,r';E) j_J(kr') G_a(r'),\\
R^m_3 &= \int drdr' r^2 r'^2 F_a(r) j_J(kr) g_{11}(r,r';E) j_J(kr') F_a(r'),\\
R^m_4 &= \int drdr' r^2 r'^2 G_a(r) j_J(kr) g_{21}(r,r';E) j_J(kr') F_a(r'),\\
R^e_{1'} &= \int drdr' r^2 r'^2 G_a(r) j_J(kr) g_{11}(r,r';E) j_J(kr') G_a(r'),\\
R^e_{2'} &= \int drdr' r^2 r'^2 F_a(r) j_J(kr) g_{21}(r,r';E) j_J(kr') G_a(r'),\\
R^e_{3'} &= \int drdr' r^2 r'^2 G_a(r) j_J(kr) g_{12}(r,r';E) j_J(kr') F_a(r'),\\
R^e_{4'} &= \int drdr' r^2 r'^2 F_a(r) j_J(kr) g_{22}(r,r';E) j_J(kr') F_a(r').
\end{aligned} \tag{29}$$

In these integrals, $j_J(kr)$ is the spherical Bessel function [24] and the g_{ij} $(i,j=1,2)$ are the radial components of the Coulomb-Dirac Green's function.

All radial matrix elements can be evaluated analytically by the help of the substitution

$$j_l(kr) = \left(\frac{\pi}{2kr}\right)^{1/2} J_{l+1/2}(kr), \tag{30}$$

and the Taylor expansion of the Bessel functions $J_{l+1/2}$:

$$j_l(kr) = \sqrt{\frac{\pi}{2kr}} \sum_{n=0} \frac{(-1)^n}{2^{2n+l+1/2} n!\Gamma(n+l+3/2)} (kr)^{2n+l+1/2}. \tag{31}$$

The final results are as follows:

$$R^m_1 = \left(1 - \frac{E_a^2}{m^2c^4}\right)^{1/2} U_a^2 \frac{1}{2} (2\lambda_n)^{(2\gamma_n)} \sum_n \left(-(\kappa_n + \nu/\epsilon_n) \frac{n!\left(I^2_{A_1J} - I^2_{B_1J}\right)}{\Gamma(2\gamma_n+1+n)(n+\gamma_n+1-\nu)} - (\kappa_n - \nu/\epsilon_n) \frac{n!\left(I^2_{A_1J} - I^2_{B_1J}\right)}{\Gamma(2\gamma_n+1+n)(n+\gamma_n-\nu)} - \frac{n!2}{\Gamma(2\gamma_n+n)(n+\gamma_n-\nu)} \left(I_{A_2J} I_{B_1J} - I_{A_1J} I_{B_2J}\right) \right), \tag{32}$$

$$R^m_2 = \left(1 + \frac{E_a}{mc^2}\right) U_a^2 \frac{\varepsilon}{2} (2\lambda_n)^{(2\gamma_n)} \sum_n \left((\kappa_n + \nu/\epsilon_n) \frac{n!'\left(I_{A_1J} - I_{B_1J}\right)^2}{\Gamma(2\gamma_n+1+n)(n+\gamma_n+1-\nu)} - [(\kappa_n - \nu/\epsilon_n) - 2(\gamma_n+\nu)] \times \frac{n!\left(I_{A_1J} - I_{B_1J}\right)^2}{\Gamma(2\gamma_n+1+n)(n+\gamma_n-\nu)} - \frac{n!2}{\Gamma(2\gamma_n+n)(n+\gamma_n-\nu)} \left(I_{A_2J} I_{A_1J} - I_{A_1J} I_{B_2J} - I_{A_2J} I_{B_1J} + I_{B_1J} I_{B_2J}\right) \right), \tag{33}$$

$$R^m_3 = \left(1 - \frac{E_a}{mc^2}\right) U_a^2 \frac{1}{2\varepsilon} (2\lambda_n)^{(2\gamma_n)} \sum_n \left((\kappa_n + \nu/\epsilon_n) \frac{n!\left(I_{A_1J} + I_{B_1J}\right)^2}{\Gamma(2\gamma_n+1+n)(n+\gamma_n+1-\nu)} - [(\kappa_n - \nu/\epsilon_n) + 2(\gamma_n+\nu)] \times \frac{n!\left(I_{A_1J} + I_{B_1J}\right)^2}{\Gamma(2\gamma_n+1+n)(n+\gamma_n-\nu)} + \frac{n!2}{\Gamma(2\gamma_n+n)(n+\gamma_n-\nu)} \left(I_{A_2J} I_{A_1J} + I_{A_1J} I_{B_2J} + I_{A_2J} I_{B_1J} + I_{B_1J} I_{B_2J}\right) \right), \tag{34}$$

$$R^m_4 = \left(1 - \frac{E_a^2}{m^2c^4}\right) U_a^2 \frac{1}{2} (2\lambda_n)^{(2\gamma_n)} \sum_n \left(- (\kappa_n + \nu/\epsilon_n) \frac{n!\left(I^2_{A_1J} - I^2_{B_1J}\right)}{\Gamma(2\gamma_n+1+n)(n+\gamma_n+1-\nu)} - (\kappa_n - \nu/\epsilon_n) \frac{n!\left(I^2_{A_1J} - I^2_{B_1J}\right)}{\Gamma(2\gamma_n+1+n)(n+\gamma_n-\nu)} - \frac{n!2}{\Gamma(2\gamma_n+n)(n+\gamma_n-\nu)} \left(I_{A_2J} I_{B_1J} - I_{A_1J} I_{B_2J}\right) \right), \tag{35}$$

$$R^e_{1'} = \left(1 + \frac{E_a}{mc^2}\right) U_a^2 \frac{1}{2\varepsilon} (2\lambda_n)^{(2\gamma_n)} \sum_n \left((\kappa_n + \nu/\epsilon_n) \frac{n!\left(I_{A_1J} - I_{B_1J}\right)^2}{\Gamma(2\gamma_n+1+n)(n+\gamma_n+1-\nu)} - [(\kappa_n - \nu/\epsilon_n) + 2(\gamma_n+\nu)] \times \frac{n!(I_{A_1J} - I_{B_1J})^2}{\Gamma(2\gamma_n+1+n)(n+\gamma_n-\nu)} + \frac{n!2}{\Gamma(2\gamma_n+n)(n+\gamma_n-\nu)} \left(I_{A_2J} I_{A_1J} - I_{A_1J} I_{B_2J} - I_{A_2J} I_{B_1J} + I_{B_1J} I_{B_2J}\right) \right), \tag{36}$$

$$R^e_{2'} = \left(1-\frac{E_a^2}{m^2c^4}\right)^{1/2} U_a^2 \frac{1}{2}(2\lambda_n)^{(2\gamma_n)} \sum_n \left(-(\kappa_n + \nu/\epsilon_n)\frac{n!\left(I^2_{A_1J} - I^2_{B_1J}\right)}{\Gamma(2\gamma_n+1+n)(n+\gamma_n+1-\nu)} \right.$$
$$\left. - (\kappa_n - \nu/\epsilon_n)\frac{n!\left(I^2_{A_1J} - I^2_{B_1J}\right)}{\Gamma(2\gamma_n+1+n)(n+\gamma_n-\nu)} + \frac{n!2}{\Gamma(2\gamma_n+n)(n+\gamma_n-\nu)}\left(I_{A_2J}I_{B_1J} - I_{A_1J}I_{B_2J}\right)\right), \tag{37}$$

$$R^e_{3'} = \left(1-\frac{E_a^2}{m^2c^4}\right)^{1/2} U_a^2 \frac{1}{2}(2\lambda_n)^{(2\gamma_n)} \sum_n (-(\kappa_n + \nu/\epsilon_n)\frac{n!\left(I^2_{A_1J} - I^2_{B_1J}\right)}{\Gamma(2\gamma_n+1+n)(n+\gamma_n+1-\nu)}$$
$$- (\kappa_n - \nu/\epsilon_n)\frac{n!\left(I^2_{A_1J} - I^2_{B_1J}\right)}{\Gamma(2\gamma_n+1+n)(n+\gamma_n-\nu)} + \frac{n!2}{\Gamma(2\gamma_n+n)(n+\gamma_n-\nu)}\left(I_{A_2J}I_{B_1J} - I_{A_1J}I_{B_2J}\right)\Big), \tag{38}$$

$$R^e_{4'} = \left(1-\frac{E_a}{mc^2}\right) U_a^2 \frac{\varepsilon}{2}(2\lambda_n)^{(2\gamma_n)} \sum_n \left((\kappa_n + \nu/\epsilon_n)\frac{n!\left(I_{A_1J} + I_{B_1J}\right)^2}{\Gamma(2\gamma_n+1+n)(n+\gamma_n+1-\nu)} - [(\kappa_n - \nu/\epsilon_n) - 2(\gamma_n+\nu)] \right.$$
$$\left. \times \frac{n!\left(I_{A_1J} + I_{B_1J}\right)^2}{\Gamma(2\gamma_n+1+n)(n+\gamma_n-\nu)} - \frac{n!2}{\Gamma(2\gamma_n+n)(n+\gamma_n-\nu)}\left(I_{A_2J}I_{A_1J} + I_{A_1J}I_{B_2J} + I_{A_2J}I_{B_1J} + I_{B_1J}I_{B_2J}\right)\right). \tag{39}$$

For the one-dimensional radial integrals we obtain the following analytical results:

$$I_{A_1J} = \left(\frac{\pi}{2k}\right)\sum_{\alpha,p} \frac{a_r(-1)^\alpha}{\alpha!\Gamma(\alpha+l+3/2)} \frac{(-a_r+1)_p}{(2\gamma_a+1)_p} \frac{\Gamma(\gamma_{\rm an}+l+2\alpha+p+1)\Gamma(2\gamma_n+n+1)}{n!\Gamma(2\gamma_n+1)}$$
$$\times \left(\frac{k}{2}\right)^{2\alpha+l+1/2} \frac{(2\lambda_a)^{p+\gamma_a-1}}{p!}\lambda_{\rm an}^{-(\gamma_{\rm an}+p+2)}\,{}_2F_1\left(-n,\gamma_{\rm an}+l+2\alpha+p+1,2\gamma_n+1,\frac{2\lambda_n}{\lambda_{\rm an}}\right), \tag{40}$$

$$I_{A_2J} = \left(\frac{\pi}{2k}\right)\sum_{\alpha,p} \frac{a_r(-1)^\alpha}{\alpha!\Gamma(\alpha+l+3/2)} \frac{(-a_r+1)_p}{(2\gamma_a+1)_p} \frac{\Gamma(\gamma_{\rm an}+l+2\alpha+p+1)\Gamma(2\gamma_n+n)}{n!\Gamma(2\gamma_n)}$$
$$\times \left(\frac{k}{2}\right)^{2\alpha+l+1/2} \frac{(2\lambda_a)^{p+\gamma_a-1}}{p!}\lambda_{\rm an}^{-(\gamma_{\rm an}+p+2)}\,{}_2F_1\left(-n,\gamma_{\rm an}+l+2\alpha+p+1,2\gamma_n,\frac{2\lambda_n}{\lambda_{\rm an}}\right), \tag{41}$$

$$I_{B_1J} = \left(\frac{\pi}{2k}\right)\sum_{\alpha,p} \frac{(N_a-\kappa_a)(-1)^\alpha}{\alpha!\Gamma(\alpha+l+3/2)} \frac{(-a_r)_p}{(2\gamma_a+1)_p} \frac{\Gamma(\gamma_{\rm an}+l+2\alpha+p+1)\Gamma(2\gamma_n+n+1)}{n!\Gamma(2\gamma_n+1)}$$
$$\times \left(\frac{k}{2}\right)^{2\alpha+l+1/2} \frac{(2\lambda_a)^{p+\gamma_a-1}}{p!}\lambda_{\rm an}^{-(\gamma_{\rm an}+p+2)}\,{}_2F_1\left(-n,\gamma_{\rm an}+l+2\alpha+p+1,2\gamma_n+1,\frac{2\lambda_n}{\lambda_{\rm an}}\right), \tag{42}$$

$$I_{B_2J} = \left(\frac{\pi}{2k}\right)\sum_{\alpha,p} \frac{(N_a-\kappa_a)(-1)^\alpha}{\alpha!\Gamma(\alpha+l+3/2)} \frac{(-a_r)_p}{(2\gamma_a+1)_p} \frac{\Gamma(\gamma_{\rm an}+l+2\alpha+p+1)\Gamma(2\gamma_n+n)}{n!\Gamma(2\gamma_n)}$$
$$\times \left(\frac{k}{2}\right)^{2\alpha+l+1/2} \frac{(2\lambda_a)^{p+\gamma_a-1}}{p!}\lambda_{\rm an}^{-(\gamma_{\rm an}+p+2)}\,{}_2F_1\left(-n,\gamma_{\rm an}+l+2\alpha+p+1,2\gamma_n,\frac{2\lambda_n}{\lambda_{\rm an}}\right). \tag{43}$$

Here we introduced the notations $\lambda_{\rm an} = \lambda_a + \lambda_n$ and $\gamma_{\rm an} = \gamma_a + \gamma_n$ for simplicity. The remaining radial matrix elements can be calculated from the ones given in Eqs. (32)–(35) by the substitutions $R^e_i = R^m_i(J \to J+1)$ for all $i \in \{1,2,3,4\}$.

B. Angular matrix elements

Equations (27) contain angular integrals of the form

$$K^{\kappa_n\kappa_a}_{JkM} = \int do_r \Omega^\dagger_{\kappa_n}(\hat{r})\hat{\sigma}\boldsymbol{Y}_{JkM}(\hat{r})\Omega_{\kappa_a}(\hat{r}). \tag{44}$$

The direct product of the spin operator $\hat{\sigma}$ and the vector spherical harmonic is a spherical tensor operator and thus its matrix element can be rewritten as

$$K^{\kappa_n\kappa_a}_{JkM} = \left\langle l_n \tfrac{1}{2} j_n \middle| T_J(Y_k\sigma_1) \middle| l_a \tfrac{1}{2} j_a \right\rangle. \tag{45}$$

The reduced matrix elements of the tensor T can be calculated using the formula

$$\left\langle l_1 \frac{1}{2} j \middle\| T_K(C_k\sigma_1) \middle\| l_1' \frac{1}{2} j' \right\rangle$$
$$= a_K(-1)^{j'-K-1/2}(2j'+1)^{1/2}\begin{pmatrix} j & j' & K \\ \frac{1}{2} & -\frac{1}{2} & 0 \end{pmatrix}, \tag{46}$$

where the coefficients are [25]

$$a_k = (\kappa-\kappa')/\sqrt{k(k+1)},$$
$$a_{k-1} = -(k+\kappa+\kappa')/\sqrt{2k(k+1)},$$
$$a_{k+1} = (k+1-\kappa-\kappa')/\sqrt{(k+1)(2k+1)}. \tag{47}$$

TABLE I. Comparison of nonrelativistic (NR) and relativistic (R) light shifts for K and L shell states in hydrogenic ions, at an optical laser frequency. E_b denotes the binding energy of the orbital and ΔE stands for the light shift contribution.

		$Z=54$		$Z=92$	
		E_b	ΔE	E_b	ΔE
NR	$1s$	−39674.2	−1.02586(−4)	−115159	−1.21763(−5)
R	$1s_{1/2}$	−41347.0	−8.17337(−5)	−132280	−5.63212(−6)
NR	$2s$	−9918.55	−2.73564(−3)	−28789.6	−3.24700(−4)
R	$2s_{1/2}$	−10443.5	−4.94986(−2)	−34215.5	−1.40870(−3)
NR	$2p$	−9918.55	−4.92415(−3)	−28789.6	−5.84460(−4)
R	$2p_{1/2}$	−10443.5	−3.17409(−3)	−34215.5	−2.17374(−4)
R	$2p_{3/2}$	−10016.7	+4.31087(−2)	−29649.8	+7.88416(−4)

For the integrals containing the scalar spherical harmonics,

$$K_{JM}^{\kappa_n\kappa_a} = \int do_r \Omega_{\kappa_n}^{\dagger}(\hat{r}) Y_{JM}(\hat{r}) \Omega_{\kappa_a}(\hat{r}) = \left\langle l_n \frac{1}{2} j_n \middle| Y_{JM} \middle| l_a \frac{1}{2} j_a \right\rangle, \quad (48)$$

one can compute the reduced matrix elements as [25]

$$\left\langle l_1 \frac{1}{2} j \middle\| C_K \middle\| l_1' \frac{1}{2} j' \right\rangle = (-1)^{j'-K-1/2}(2j'+1)^{1/2} \begin{pmatrix} j & j' & K \\ \frac{1}{2} & -\frac{1}{2} & 0 \end{pmatrix}. \quad (49)$$

IV. NUMERICAL RESULTS

In Eq. (14), the series over intermediate states include the bound states, the positive-energy-continuum eigenstates, and also the negative-energy-continuum eigenstates. In order to evaluate these second-order expressions, we have used the Green's function in the Sturmian representation [26], in which the continuous sum over wave functions will be replaced by discrete summations running over all, positive and negative, integers. The technical procedure for transforming sums into expressions that contain only summations over non-negative integers is also presented in [26]. To obtain an accuracy of five decimal places, the number of terms included varies from 5 for $Z=26$ to 10 for $Z=91$.

TABLE III. Comparison of nonrelativistic (NR) and relativistic (R) light shifts for $1s-ns$ for Z=1, with the photon frequency equal to half of the transition frequency.

$Z=1$	$\beta_{\rm NR}$ [Hz(W/m^2)$^{-1}$] $1s-ns$	$\beta_{\rm R}$ [Hz(W/m^2)$^{-1}$] $1s_{1/2}-ns_{1/2}$
$1s-2s$	−2.67827(−5)	−2.67808(−5)
$1s-3s$	−3.02104(−5)	−3.02082(−5)
$1s-4s$	−3.18301(−5)	−3.18278(−5)
$1s-5s$	−3.26801(−5)	−3.26778(−5)
$1s-6s$	−3.31724(−5)	−3.31701(−5)
$1s-7s$	−3.34805(−5)	−3.34781(−5)
$1s-8s$	−3.36851(−5)	−3.36827(−5)
$1s-9s$	−3.38277(−5)	−3.38252(−5)

To start our discussion on relativistic results on light shifts, we present results for an atom in a laser field at an optical frequency ($\lambda = 1054$ nm, $\hbar\omega = 1.176$ eV) and with the widely accessible intensity of $I = 10^{18}$ W/cm^2. We calculate the light shifts in eV, both in relativistic and nonrelativistic treatments, for some heavy elements ($Z = 54$, 92, i.e., Xe and U). Results are shown in Table I. As it is well known, the ac Stark shifts, calculated in a nonrelativistic way, follow an exact $\propto Z^{-4}$ scaling. It is also intuitively understandable that external field effects in general have a smaller effect if the electrons are bound by stronger central potentials. Still, even for elements as heavy as Xe and U, and for orbitals of the L shell, the light shift exceeds or approaches to the meV range. This is anticipated to be noticeable in near-future experiments. For measurements with lighter elements, the effects are certainly more pronounced.

As the table also clearly shows, the relativistic and nonrelativistic results greatly differ. For these relativistic systems, the nonrelativistic calculation can only serve as an order-of-magnitude approximation, since not even the first digits of the results calculated in the two different approaches agree. In some cases, e.g., for the $2p_{3/2}$ state, even the sign of the shift is different, which is originated in the different level structure as described by the relativistic theory.

For soft x-ray frequencies ($\hbar\omega = 50$ eV), for the same intensity, we give the shifts for the elements $Z = 10$, 54, and 92 in Table II. At the heaviest system studied, namely, for U, these results almost coincide with the light shifts calculated with optical laser frequencies. This illustrates that retardation

TABLE II. Comparison of nonrelativistic (NR) and relativistic (R) light shifts for K and L shell states in hydrogenic ions at a soft x-ray laser frequency. Notations as in Table I.

		$Z=10$		$Z=54$		$Z=92$	
		E_b	ΔE	E_b	ΔE	E_b	ΔE
NR	$1s$	−1360.57	−8.74042(−2)	−39674.2	−1.02587(−4)	−115159	−1.21763(−5)
R	$1s_{1/2}$	−1362.39	−8.6767(−2)	−41347.0	−8.17339(−5)	−132280	−5.63212(−6)
NR	$2s$	−340.142	−2.47409	−9918.55	−2.73583(−3)	−28789.6	−3.24703(−4)
R	$2s_{1/2}$	−340.710	−2.33842	−10443.5	−5.01577(−2)	−34215.5	−1.40885(−3)
NR	$2p$	−340.142	−4.47426	−9918.55	−4.92452(−3)	−28789.6	−5.84465(−4)
R	$2p_{1/2}$	−340.710	−3.61534	−10443.5	−3.17429(−3)	−34215.5	−2.17375(−4)
R	$2p_{3/2}$	−340.256	−4.16667	−10016.7	+4.37674(−2)	−29649.8	+7.88564(−4)

TABLE IV. Same as Table III, but for Z=10.

$Z = 10$	$\beta_{\rm NR}$ [Hz(W/m^2)$^{-1}$] $1s - ns$	$\beta_{\rm R}$ [Hz(W/m^2)$^{-1}$] $1s_{1/2} - ns_{1/2}$
$1s - 2s$	−2.67827(−9)	−2.65885(−9)
$1s - 3s$	−3.02104(−9)	−2.99941(−9)
$1s - 4s$	−3.18301(−9)	−3.16030(−9)
$1s - 5s$	−3.26801(−9)	−3.24471(−9)
$1s - 6s$	−3.31724(−9)	−3.29360(−9)
$1s - 7s$	−3.34805(−9)	−3.32418(−9)
$1s - 8s$	−3.36851(−9)	−3.34449(−9)
$1s - 9s$	−3.38277(−9)	−3.35863(−9)

effects are only relevant when the photon energy is comparable to the atomic binding energy: in the case of U, where the binding energies exceed the 10-keV range, even a photon frequency of 50 eV is negligible in the description of the dynamic Stark shift. However, for lighter systems such as Xe ($Z = 54$), the difference between the optical and the soft x-ray light field is noticeable. This is especially the case for excited states.

In order to avoid a discussion about the intensity I and for a better comparison with existing nonrelativistic literature data, in the following we introduce the dynamic Stark shift coefficient β:

$$\Delta E = h\beta I, \tag{50}$$

where ΔE is the Stark shift of the atomic level $|\Phi_a\rangle$. In Tables III, IV, and V, the nonrelativistic and relativistic Stark shift coefficients β_{NR} and β_R are compared for the half $1s - ns$ transition frequency for nuclear charge numbers $Z = 1$, 10, and 54. The light shift calculated in the nonrelativistic limit of the formulas derived in this paper agrees perfectly with the calculations of Haas [14]. Also, they show an exact $\propto Z^{-4}$ scaling with the atomic number Z. However, for the relativistic results, a clear deviation from this law is observable, especially for the highest atomic charge numbers. These tables also illustrate that the light shifts are most relevant for highly excited, weakly bound states, i.e., for Rydberg levels.

As we can see from Eqs. (22) and (25), in the final expression of dipole light shifts we have the following possible combinations of electromagnetic potentials: matrix elements of scalar-scalar, vector-vector, and scalar-vector potentials.

TABLE V. Same as Table III, but for Z=54.

$Z = 54$	$\beta_{\rm NR}$ [Hz(W/m^2)$^{-1}$] $1s - ns$	$\beta_{\rm R}$ [Hz(W/m^2)$^{-1}$] $1s_{1/2} - ns_{1/2}$
$1s - 2s$	−3.14978(−12)	−2.51398(−12)
$1s - 3s$	−3.55288(−12)	−2.84491(−12)
$1s - 4s$	−3.74337(−12)	−3.00038(−12)
$1s - 5s$	−3.84334(−12)	−3.08132(−12)
$1s - 6s$	−3.90124(−12)	−3.12789(−12)
$1s - 7s$	−3.93747(−12)	−3.15688(−12)
$1s - 8s$	−3.96153(−12)	−3.17606(−12)
$1s - 9s$	−3.97829(−12)	−3.18937(−12)

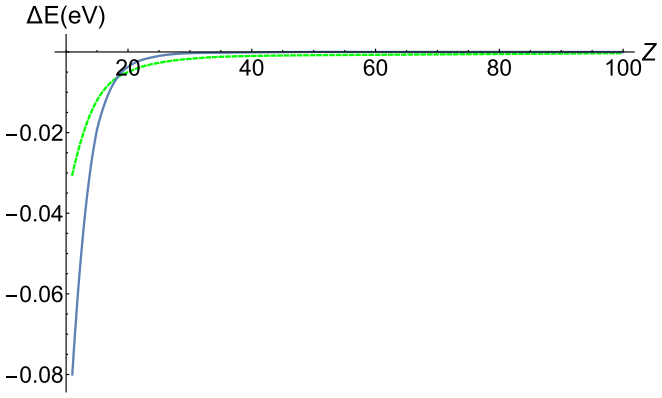

FIG. 2. Light shift of the $1s_{1/2}$ energy levels in a hydrogenlike ion as a function of the charge number Z, for a laser intensity of $I = 10^{18}$ W/cm^2. The E_1 (blue, continuous) and 1000 times the contribution of M_1 (dashed, green) are shown.

Because of the selection rules incorporated in the angular matrix elements, the scalar-vector part is zero. In the following tables we give some values of the dynamic Stark shift coefficient β for scalar-scalar and vector-vector parts and for the interaction with the magnetic-field component of the laser field, including the retardation contribution caused by the dependence on the photon frequency. The tables show that the scalar-scalar contribution is by far the dominant part of the interaction.

In Fig. 2, we represented the light shift of the $1s_{1/2}$ energy levels in a hydrogenlike ion as a function of the charge number Z, for a laser intensity of $I = 10^{18}$ W/cm^2. We represented both the contribution of E_1 and 1000 times the contribution of M_1. In Fig. 3, we represented the light shift of the $1s_{1/2}$ energy levels in a hydrogenlike ion as a function of the charge number Z, for the same setup as the one in Fig. 2. The E_1 and M_1 contributions are shown.

Taking into account the fact that only the scalar-scalar part contributes, the Breit-Pauli approximation should be sufficient [14]. In Tables VI and VII we can see the retardation contribution compared to the Breit-Pauli approximation. Developing the electromagnetic field in multipoles, we obtain important contributions to the resonance. When the photon

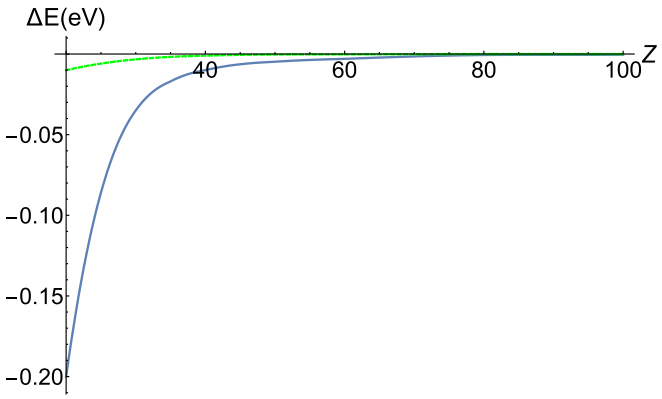

FIG. 3. The same setup as in Fig. 2, for $2p_{1/2}$. The E_1 (blue, continuous) and M_1 (dashed, green) contributions are shown.

TABLE VI. Different relativistic electric dipole (E_1) contributions to the light shift for $1s - ns$ two-photon transitions: scalar-scalar (s-s), vector-vector (v-v), and magnetic-field contributions, with or without frequency-dependent retardation (ret.) contributions. The results are given for $Z = 10$.

$Z = 10$	s-s	s-s, ret.	v-v	v-v, ret.	Mag.	Mag., ret.
$1s - 2s$	−2.6588(−9)	−2.6579(−9)	−6.7879(−16)	−6.7848(−16)	−9.2665(−13)	−9.2635(−13)
$1s - 3s$	−2.9994(−9)	−2.9978(−9)	−1.0200(−15)	−1.0193(−15)	−1.0973(−12)	−1.0968(−12)
$1s - 4s$	−3.1603(−9)	−3.1584(−9)	−1.1667(−15)	−1.1658(−15)	−1.1753(−12)	−1.1746(−12)
$1s - 5s$	−3.2447(−9)	−3.2427(−9)	−1.2402(−15)	−1.2393(−15)	−1.2156(−12)	−1.2149(−12)
$1s - 6s$	−3.2936(−9)	−3.2915(−9)	−1.2818(−15)	−1.2808(−15)	−1.2387(−12)	−1.2380(−12)
$1s - 7s$	−3.3241(−9)	−3.3220(−9)	−1.3075(−15)	−1.3064(−15)	−1.2531(−12)	−1.2524(−12)
$1s - 8s$	−3.3444(−9)	−3.3423(−9)	−1.3243(−15)	−1.3233(−15)	−1.2627(−12)	−1.2619(−12)
$1s - 9s$	−3.3586(−9)	−3.3564(−9)	−1.3360(−15)	−1.3349(−15)	−1.2693(−12)	−1.2685(−12)

frequency is equal to half of the transition frequency, the Stark shift comes from the E_1 transitions. One may conclude that the dipole approximation is good, especially for low charge states where the retardation effect is small. At high nuclear charges and frequencies, the dependence of the scalar-scalar term on the photon frequency starts to show up; however, the vector-vector and magnetic terms are still orders of magnitude smaller.

V. SUMMARY

Off-resonant light shifts of hydrogenic levels are calculated in a fully relativistic framework. We used Coulomb-Dirac wave functions and Green's functions in the Sturmian representation to evaluate the second-order expressions. The electromagnetic field has been expanded into multipoles, which enabled us to study the nondipole effects of interaction with magnetic-field components of the laser light and retardation contributions depending on the frequency of the laser photon. At high laser intensities, the light shifts are sizable, especially for excited states with lower binding energies. These results are relevant in current and near-future spectroscopic experiments, especially for experiments employing advanced light sources in the x-ray regime.

ACKNOWLEDGMENTS

The author acknowledges helpful conversations with Zoltan Harman, Christoph H. Keitel, and Flavius Dragoi.

APPENDIX A: COULOMB-DIRAC GREEN'S FUNCTION IN THE STURMIAN REPRESENTATION

Given a Hermitian operator H, the corresponding resolvent or Green operator $G(z)$ is defined by

$$(H - z)G(z) = 1, \tag{A1}$$

where z, referred to later on as the *energy variable*, is a complex number. Let us assume that H possesses a complete set of eigenfunctions Φ_n corresponding to eigenvalues E:

$$(H - E_n)\Phi_n = 0, \tag{A2}$$

$$\sum_n \Phi_n \Phi_n^\dagger = 1. \tag{A3}$$

In the spectral representation, $G(z)$ is formally given by

$$G(z) = -\sum_n \frac{\Phi_n \Phi_n^\dagger}{z - E_n}. \tag{A4}$$

Generally, the summation is performed over a discrete and a continuous spectrum of eigenfunctions.

If H is represented by a differential operator H_r acting on a Hilbert space of functions on R^3, $G(z)$ is itself represented by a function $G(\boldsymbol{r_1}, \boldsymbol{r_2}; z)$ on $R^3 \times R^3$ which satisfies the equation

$$(H_{r_1} - z)G(\boldsymbol{r_1}, \boldsymbol{r_2}; z) = \delta(\boldsymbol{r_1} - \boldsymbol{r_2}). \tag{A5}$$

For a certain class of Hamiltonians, the Green's function can be given analytically, without explicitly carrying out the summation over a complete spectrum. The Green's function

TABLE VII. Same as Table VI, for $Z = 54$.

$Z = 54$	s-s	s-s, ret.	v-v	v-v, ret.	Mag.	Mag., ret.
$1s - 2s$	−2.5139(−12)	−2.4873(−12)	−6.2890(−16)	−6.2032(−16)	−2.8362(−14)	−2.8093(−14)
$1s - 3s$	−2.8449(−12)	−2.8013(−12)	−9.5338(−16)	−9.3473(−16)	−3.3758(−14)	−3.3284(−14)
$1s - 4s$	−3.0003(−12)	−2.9488(−12)	−1.0922(−15)	−1.0683(−15)	−3.6223(−14)	−3.5646(−14)
$1s - 5s$	−3.0813(−12)	−3.0255(−12)	−1.1615(−15)	−1.1347(−15)	−3.7490(−14)	−3.6859(−14)
$1s - 6s$	−3.1278(−12)	−3.0697(−12)	−1.2004(−15)	−1.1720(−15)	−3.8214(−14)	−3.7552(−14)
$1s - 7s$	−3.1568(−12)	−3.0972(−12)	−1.2243(−15)	−1.1949(−15)	−3.8664(−14)	−3.7982(−14)
$1s - 8s$	−3.1760(−12)	−3.1153(−12)	−1.2400(−15)	−1.2099(−15)	−3.8960(−14)	−3.8266(−14)
$1s - 9s$	−3.1893(−12)	−3.1280(−12)	−1.2508(−15)	−1.2202(−15)	−3.9166(−14)	−3.8462(−14)

associated with the Dirac-Coulomb Hamiltonian can be decomposed into radial and angular parts as

$$G(\boldsymbol{r}_1, \boldsymbol{r}_2; E_n) = \frac{1}{c\hbar}\begin{pmatrix} G^{11} & G^{12} \\ G^{21} & G^{22} \end{pmatrix}, \tag{A6}$$

where in the components G^{ij}, $i, j \in \{1, 2\}$, which are 2×2 matrices, we omitted the coordinate and energy arguments for brevity. They can be decomposed as

$$G^{11} = \sum_{\kappa_n m_n} g^{11}_{\kappa_n}(r_1, r_2; E_n)\Omega_{\kappa_n m_n}(\hat{r})\Omega^*_{\kappa_n m_n}(\hat{r'}),$$
$$G^{12} = \sum_{\kappa_n m_n} -ig^{12}_{\kappa_n}(r_1, r_2; E_n)\Omega_{\kappa_n m_n}(\hat{r})\Omega^*_{-\kappa_n m_n}(\hat{r'}),$$
$$G^{21} = \sum_{\kappa_n m_n} ig^{21}_{\kappa_n}(r_1, r_2; E_n)\Omega_{-\kappa_n m_n}(\hat{r})\Omega^*_{\kappa_n m_n}(\hat{r'}),$$
$$G^{22} = \sum_{\kappa_n m_n} g^{22}_{\kappa_n}(r_1, r_2; E_n)\Omega_{-\kappa_n m_n}(\hat{r})\Omega^*_{-\kappa_n m_n}(\hat{r'}). \tag{A7}$$

The radial components g^{ij} can be represented as an expansion involving Laguerre polynomials. Introducing the notations

$$\varepsilon = \sqrt{\frac{mc^2 - E}{mc^2 + E}}, \epsilon = \frac{E}{mc^2}, \nu = \frac{\alpha Z \epsilon}{\sqrt{1-\epsilon^2}}, \tag{A8}$$

the explicit formulas for the radial components are [26]

$$g^{11}_{\kappa_n} = \frac{1}{2\varepsilon}(2\lambda_n)^{2\gamma_n}(rr')^{\gamma_n - 1}e^{-\lambda_n(r+r')}\sum_{n=0}^{\infty}\left((\kappa_n + \nu/\epsilon_n)\frac{n!}{\Gamma(2\gamma_n + 1 + n)}\frac{L_n^{2\gamma_n}(2\lambda_n r)L_n^{2\gamma_n}(2\lambda_n r')}{n + \gamma_n + 1 - \nu} - [(\kappa_n - \nu/\epsilon_n) + 2(\gamma_n + \nu)]\right.$$
$$\left.\times\frac{n!}{\Gamma(2\gamma_n + 1 + n)}\frac{L_n^{2\gamma_n}(2\lambda_n r)L_n^{2\gamma_n}(2\lambda_n r')}{n + \gamma_n - \nu} + \frac{n!}{\Gamma(2\gamma_n + n)}\frac{L_n^{2\gamma_n - 1}(2\lambda_n r)L_n^{2\gamma_n}(2\lambda_n r') + L_n^{2\gamma_n}(2\lambda_n r)L_n^{2\gamma_n - 1}(2\lambda_n r')}{n + \gamma_n - \nu}\right), \tag{A9}$$

$$g^{12}_{\kappa_n} = \frac{1}{2}(2\lambda_n)^{2\gamma_n}(rr')^{\gamma_n - 1}e^{-\lambda_n(r+r')}\sum_{n=0}^{\infty}\left((\kappa_n + \nu/\epsilon_n)\frac{n!}{\Gamma(2\gamma_n + 1 + n)}\frac{L_n^{2\gamma_n}(2\lambda_n r)L_n^{2\gamma_n}(2\lambda_n r')}{n + \gamma_n + 1 - \nu} + (\kappa_n - \nu/\epsilon_n)\frac{n!}{\Gamma(2\gamma_n + 1 + n)}\right.$$
$$\left.\times\frac{L_n^{2\gamma_n}(2\lambda_n r)L_n^{2\gamma_n}(2\lambda_n r')}{n + \gamma_n - \nu} - \frac{n!}{\Gamma(2\gamma_n + n)}\frac{L_n^{2\gamma_n - 1}(2\lambda_n r)L_n^{2\gamma_n}(2\lambda_n r') - L_n^{2\gamma_n}(2\lambda_n r)L_n^{2\gamma_n - 1}(2\lambda_n r')}{n + \gamma_n - \nu}\right), \tag{A10}$$

$$g^{21}_{\kappa_n} = g^{12}_{\kappa_n}(r \leftrightarrow r'), \tag{A11}$$

$$g^{22}_{\kappa_n} = \frac{\varepsilon}{2}(2\lambda_n)^{2\gamma_n}(rr')^{\gamma_n - 1}e^{-\lambda_n(r+r')}\sum_{n=0}^{\infty}\left((\kappa_n + \nu/\epsilon_n)\frac{n!}{\Gamma(2\gamma_n + 1 + n)}\frac{L_n^{2\gamma_n}(2\lambda_n r)L_n^{2\gamma_n}(2\lambda_n r')}{n + \gamma_n + 1 - \nu} - [(\kappa_n - \nu/\epsilon_n) - 2(\gamma_n + \nu)]\right.$$
$$\left.\times\frac{n!}{\Gamma(2\gamma_n + 1 + n)}\frac{L_n^{2\gamma_n}(2\lambda_n r)L_n^{2\gamma_n}(2\lambda_n r')}{n + \gamma_n - \nu} - \frac{n!}{\Gamma(2\gamma_n + n)}\frac{L_n^{2\gamma_n - 1}(2\lambda_n r)L_n^{2\gamma_n}(2\lambda_n r') + L_n^{2\gamma_n}(2\lambda_n r)L_n^{2\gamma_n - 1}(2\lambda_n r')}{n + \gamma_n - \nu}\right). \tag{A12}$$

APPENDIX B: ELECTROMAGNETIC MULTIPOLES

In the following, we systematize the decomposition of the first-order transition amplitude into multipole components (electric and magnetic dipole, electric and magnetic quadrupole, etc.). The transition matrix element is defined as

$$T_{\rm an} = \int d^3 r \phi_a^\dagger(\mathbf{r})\boldsymbol{\alpha}\mathbf{A}(\mathbf{r}, \omega)\phi_n(\mathbf{r}), \tag{B1}$$

where $\boldsymbol{A}(\boldsymbol{r}, \omega)$ is the transverse-gauge vector potential [19]:

$$\boldsymbol{A}(\boldsymbol{r}, \omega) = \hat{\epsilon}e^{i\boldsymbol{kr}}. \tag{B2}$$

As a first step of the multipole decomposition, we expand the vector potential $\boldsymbol{A}(\boldsymbol{r}, \omega)$ in a series of vector spherical harmonics [19] as

$$\boldsymbol{A}(\boldsymbol{r}, \omega) = \sum_{JLM} A_{JLM}\boldsymbol{Y}_{JLM}(\hat{r}). \tag{B3}$$

The expansion coefficients are given by

$$A_{JLM} = \int d\Omega[\boldsymbol{Y}_{JLM}(\hat{r}) \cdot \hat{\epsilon}]^\dagger e^{i\boldsymbol{kr}}. \tag{B4}$$

Using the expansion of a plane wave in terms of spherical Bessel functions $j_l(kr)$ [24], namely,

$$e^{i\boldsymbol{kr}} = 4\pi\sum_{lm} i^l j_l(kr)Y^*_{lm}(\hat{k})Y_{lm}(\hat{r}), \tag{B5}$$

and carrying out the angular integration in Eq. (B4), we can rewrite the vector potential in the form

$$\boldsymbol{A}(\boldsymbol{r}, \omega) = 4\pi\sum_{JLM} i^L[\boldsymbol{Y}_{JLM}(\hat{k}) \cdot \hat{\epsilon}]\boldsymbol{a}_{JLM}(\boldsymbol{r}), \tag{B6}$$

with

$$\boldsymbol{a}_{JLM}(\boldsymbol{r}) = j_L(kr)\boldsymbol{Y}_{JLM}(\hat{r}). \tag{B7}$$

For compactness, we introduce the notation $\boldsymbol{Y}^{(\lambda)}_{JM}(\hat{r})$, which is related to the vector spherical harmonics as

$$\boldsymbol{Y}_{JJ-1M}(\hat{r}) = \sqrt{\frac{J}{2J+1}}\boldsymbol{Y}^{(-1)}_{JM}(\hat{r}) + \sqrt{\frac{J+1}{2J+1}}\boldsymbol{Y}^{(1)}_{JM}(\hat{r}),$$
$$\boldsymbol{Y}_{JJM}(\hat{r}) = \boldsymbol{Y}^{(0)}_{JM}(\hat{r}), \tag{B8}$$
$$\boldsymbol{Y}_{JJ+1M}(\hat{r}) = -\sqrt{\frac{J+1}{2J+1}}\boldsymbol{Y}^{(-1)}_{JM}(\hat{r}) + \sqrt{\frac{J}{2J+1}}\boldsymbol{Y}^{(1)}_{JM}(\hat{r}).$$

This transformation leads immediately to the multipole expansion of the vector potential:

$$\boldsymbol{A}(\boldsymbol{r},\omega) = 4\pi \sum_{JM\lambda} i^{J-\lambda} [\boldsymbol{Y}_{JM}^{(\lambda)}(\hat{k}) \cdot \hat{\epsilon}]^{\dagger} \boldsymbol{a}_{JM}^{(\lambda)}(\boldsymbol{r}). \tag{B9}$$

The vector functions $\boldsymbol{a}_{JM}^{(\lambda)}$ are referred to as the multipole potentials. They are given by

$$\begin{aligned} \boldsymbol{a}_{JM}^{(0)}(\boldsymbol{r}) &= \boldsymbol{a}_{JJM}(\boldsymbol{r}), \\ \boldsymbol{a}_{JM}^{(1)}(\boldsymbol{r}) &= \sqrt{\frac{J+1}{2J+1}} \boldsymbol{a}_{JJ-1M}(\boldsymbol{r}) - \sqrt{\frac{J}{2J+1}} \boldsymbol{a}_{JJ+1M}(\boldsymbol{r}). \end{aligned} \tag{B10}$$

Only terms with $\lambda = 0$ and 1 contribute to this multipole expansion, since $\boldsymbol{Y}_{JM}^{(-1)}(\hat{k}) = \hat{k} Y_{JM}(\hat{k})$ is orthogonal to $\hat{k}$.

A gauge transformation leaves the transition amplitudes invariant, provided the energy difference between the initial and final states equals the energy carried off by the photon. The transformed multipole potential can be written as

$$\begin{aligned} \boldsymbol{a}_{JM}^{\lambda}(\hat{r}) &\longrightarrow \boldsymbol{a}_{JM}^{\lambda}(\hat{r}) + \nabla \chi_{JM}(\hat{r}), \\ \Phi_{JM}(\hat{r}) &\longrightarrow i\omega \chi_{JM}(\hat{r}), \end{aligned} \tag{B11}$$

where the gauge function $\chi_{JM}(\hat{r})$ is a solution to the Helmholtz equation. We choose the gauge function to be

$$\chi_{JM}(\hat{r}) = -\frac{1}{k} \sqrt{\frac{J+1}{J}} j_J(kr) Y_{JM}(\hat{r}), \tag{B12}$$

to cancel the contribution that is of lowest order in powers of kr. The resulting transformation has no effect on the magnetic multipoles, but transforms electric multipole potentials to the form

$$\begin{aligned} \boldsymbol{a}_{JM}^{(1)}(\hat{r}) &= -j_{J+1}(kr) \left(\boldsymbol{Y}_{JM}^{(1)}(\hat{r}) - \sqrt{\frac{J+1}{J}} \boldsymbol{Y}_{JM}^{(-1)}(\hat{r}) \right), \\ \Phi_{JM}^{(1)}(\hat{r}) &= -ic \sqrt{\frac{J+1}{J}} j_J(kr) Y_{JM}(\hat{r}). \end{aligned} \tag{B13}$$

The resulting potentials reduce to the *length form* potentials in the nonrelativistic limit [21,22].

[1] T. W. Hänsch and H. Walther, Rev. Mod. Phys. **71**, S242 (1999).
[2] T. Udem, R. Holzwarth, and T. W. Hänsch, Nature (London) **416**, 233 (2002).
[3] T. Steinmetz, T. Wilken, C. Araujo-Hauck, R. Holzwarth, T. W. Hänsch, L. Pasquini, A. Manescau, S. D'Odorico, M. T. Murphy, Th. Kentischer, W. Schmidt, and Th. Udem, Science **321**, 1335 (2008).
[4] R. Sánchez, W. Nörtershäuser, G. Ewald, D. Albers, J. Behr, P. Bricault, B. A. Bushaw, A. Dax, J. Dilling, M. Dombsky, G. W. F. Drake, S. Gotte, R. Kirchner, H. J. Kluge, T. Kuhl, J. Lassen, C. D. P. Levy, M. Pearson, E. Prime, V. Ryjkov, A. Wojtaszek, Z. C. Yan, and C. Zimmermann, Phys. Rev. Lett. **96**, 033002 (2006).
[5] W. Geithner, T. Neff, G. Audi, K. Blaum, P. Delahaye, H. Feldmeier, S. George, C. Guénaut, F. Herfurth, A. Herlert *et al.*, Phys. Rev. Lett. **101**, 252502 (2008).
[6] S. Liu, Y. Zhang, C. Yang, S. Liu, Z. Ge, Y. Li, Y. Li, Z. Zhou, G. Guo, and B. Shi, Phys. Rev. A **101**, 052324 (2020).
[7] A. Anikin, T. Zalialiutdinov, and D. Solovyev, Phys. Rev. A **103**, 022833 (2021).
[8] K. S. Rajasree, R. K. Gupta, V. Gokhroo, F. Le Kien, T. Nieddu, T. Ray, S. Nic Chormaic, and G. Tkachenko, Phys. Rev. Res. **2**, 033341 (2020).
[9] F. Zou, X.-Y. Zhang, X.-W. Xu, J.-F. Huang, and J.-Q. Liao, Phys. Rev. A **102**, 053710 (2020).
[10] A. A. Sorokin, S. V. Bobashev, T. Feigl, K. Tiedtke, H. Wabnitz, and M. Richter, Phys. Rev. Lett. **99**, 213002 (2007).
[11] J. T. Costello, J. Phys.: Conf. Ser. **88**, 012057 (2007).
[12] M. Klaiber, K. Z. Hatsagortsyan, and C. H. Keitel, Phys. Rev. A **73**, 053411 (2006).
[13] M. Haas, U. D. Jentschura, C. H. Keitel, N. Kolachevsky, M. Herrmann, P. Fendel, M. Fischer, T. Udem, R. Holzwarth, T. W. Hänsch *et al.*, Phys. Rev. A **73**, 052501 (2006).
[14] M. Haas, Ph.D. thesis, Ruperto-Carola University of Heidelberg, Germany, 2006.
[15] R. Szmytkowski, Phys. Rev. A **65**, 012503 (2001).
[16] S. W. Epp, J. R. Crespo López-Urrutia, G. Brenner, V. Mäckel, P. H. Mokler, R. Treusch, M. Kuhlmann, M. V. Yurkov, J. Feldhaus, J. R. Schneider, M. Wellhofer, M. Martins, W. Wurth, and J. Ullrich, Phys. Rev. Lett. **98**, 183001 (2007).
[17] J. J. Sakurai, *Modern Quantum Mechanics* (Addison-Wesley, Reading, MA, 1994).
[18] B. M. Brandsenand C. J. Joachain, *Introduction to Quantum Mechanics* (Longmans, Green, New York, 1989).
[19] W. R. Johnson, *Atomic Structure Theory: Lectures on Atomic Physics* (Springer, New York, 2007).
[20] A. O. Barutand Y. I. Salamin, Phys. Rev. A **37**, 2284 (1988).
[21] I. P. Grant, J. Phys. B **7**, 1458 (1974).
[22] I. P. Grant, *Relativistic Quantum Theory of Atoms and Molecules: Theory and Computation* (Springer, New York, 2007).
[23] F. A. Babushkin, Opt. Spectr. **13**, 77 (1962).
[24] M. Abramowitz and I. A. Stegun, *Handbook of Mathematical Functions*, Applied Mathematics Series, Vol. 55 (National Bureau of Standards, 1972).
[25] D. M. Brinkand G. R. Satchler, *Angular Momentum* (Oxford University, New York, 2002).
[26] R. Szmytkowski, J. Phys. B: At., Mol. Opt. Phys. **30**, 825 (1997).